

Arsenic Trioxide Sensitizes Glioblastoma to a Myc Inhibitor

著者	Yoshimura Yayoi
journal or publication title	PLoS ONE
volume	10
number	6
page range	e0128288
year	2015-06-03
学位授与機関	滋賀医科大学
学位授与番号	14202乙第424号
URL	http://hdl.handle.net/10422/00012288

doi: 10.1371/journal.pone.0128288

RESEARCH ARTICLE

Arsenic Trioxide Sensitizes Glioblastoma to a Myc Inhibitor

Yayoi Yoshimura^{1,4}, Akihiko Shiino^{3,4}, Kazue Muraki¹, Tadateru Fukami⁴, Shigeki Yamada², Takeshi Satow², Miyuki Fukuda², Masaaki Saiki², Masato Hojo², Susumu Miyamoto⁵, Nobuyuki Onishi⁶, Hideyuki Saya⁶, Toshiro Inubushi³, Kazuhiko Nozaki^{4*}, Kenji Tanigaki^{1*}

1 Research Institute, Shiga Medical Center, Moriyama 5-4-30, Shiga 524–8524, Japan, **2** Department of Neurosurgery, Shiga Medical Center, Shiga 524–8524, Japan, **3** Biomedical MR Science Center, Shiga University of Medical Science, Shiga 520–2192, Japan, **4** Department of Neurosurgery, Shiga University of Medical Science, Shiga 520–2192, Japan, **5** Department of Neurosurgery, Graduate School of Medicine, Kyoto University, Kyoto 606–8507, Japan, **6** Division of Gene Regulation, School of Medicine, Keio University, Tokyo 160–8582, Japan

☞ These authors contributed equally to this work.

* noz@belle.shiga-med.ac.jp (KN); tanigaki@res.med.shiga-pref.jp (KT)



CrossMark
click for updates

OPEN ACCESS

Citation: Yoshimura Y, Shiino A, Muraki K, Fukami T, Yamada S, Satow T, et al. (2015) Arsenic Trioxide Sensitizes Glioblastoma to a Myc Inhibitor. PLoS ONE 10(6): e0128288. doi:10.1371/journal.pone.0128288

Academic Editor: Ichiro Nakano, The Ohio State University, UNITED STATES

Received: July 15, 2014

Accepted: April 27, 2015

Published: June 3, 2015

Copyright: © 2015 Yoshimura et al. This is an open access article distributed under the terms of the [Creative Commons Attribution License](https://creativecommons.org/licenses/by/4.0/), which permits unrestricted use, distribution, and reproduction in any medium, provided the original author and source are credited.

Data Availability Statement: All relevant data are within the paper and its Supporting Information files.

Funding: This work was supported by Sagawa Foundation (K.T.) and Yasuda Medical Foundation (K.T.). The funders had no role in study design, data collection and analysis, decision to publish, or preparation of the manuscript.

Competing Interests: The authors have declared that no competing interests exist.

Abstract

Glioblastoma multiforme (GBM) is associated with high mortality due to infiltrative growth and recurrence. Median survival of the patients is less than 15 months, increasing requirements for new therapies. We found that both arsenic trioxide and 10058F4, an inhibitor of Myc, induced differentiation of cancer stem-like cells (CSC) of GBM and that arsenic trioxide drastically enhanced the anti-proliferative effect of 10058F4 but not apoptotic effects. EGFR-driven genetically engineered GBM mouse model showed that this cooperative effect is higher in EGFRvIII-expressing *INK4a/Arf*^{-/-} neural stem cells (NSCs) than in control wild type NSCs. In addition, treatment of GBM CSC xenografts with arsenic trioxide and 10058F4 resulted in significant decrease in tumor growth and increased differentiation with concomitant decrease of proneural and mesenchymal GBM CSCs *in vivo*. Our study was the first to evaluate arsenic trioxide and 10058F4 interaction in GBM CSC differentiation and to assess new opportunities for arsenic trioxide and 10058F4 combination as a promising approach for future differentiation therapy of GBM.

Introduction

Glioblastoma multiforme (GBM) is one of the most common malignant primary brain tumors in adult and highly resistant to conventional chemotherapy [1,2]. Constitutive-active mutation of EGFR (EGFRvIII) and loss of *CDKN2a* (*INK4a/Arf*) are often observed in GBM [3–7]. Constitutive EGFR activation is sufficient to transform *INK4a/Arf*-deficient neural stem cells (NSCs) and astrocytes into cancer stem-like cells (CSCs), which has high tumorigenicity *in vivo* [8]. GBM CSCs are considered to be an origin of tumor and recurrence [9] and are an important therapeutic target. CSCs can be cultured in serum-free medium supplemented with

bFGF and EGF in sphere conditions [10]. When transplanted to immunodeficient mice, CSCs gave rise to high-grade gliomas with pathological phenotypes more similar to GBM compared with GBM cells cultured in serum-containing media [10].

Arsenic trioxide (As_2O_3) is used for treatment of acute promyelocytic leukemia (APL), which causes the induction of differentiation of leukemic cells [11,12]. Arsenic trioxide has been reported to inhibit but not regress the growth of a wide variety of solid tumors including GBM at a clinically safety dose (1–2 μ M). Higher concentrations (10–50 μ M) are required to induce apoptosis [13–18]. 4 μ M arsenic trioxide reduces the number of CSCs of GBM, whereas the low concentrations of arsenic trioxide only inhibits renewal of CSCs without affecting properties as CSCs [18]. Thus, new method to enhance its efficacy requires to be exploited. Another candidate target of GBM therapy is c-Myc, which is also required for the maintenance of CSC of various cancers [19]. We show here that a low concentration (2 μ M) of arsenic trioxide could induce differentiation of GBM CSCs and enhanced the effect of 10058F4, a Myc inhibitor. This interaction was greater in EGFRvIII-expressing *INK4a/Arf*-deficient neural stem cells (NSCs) than in wild type NSCs, which suggests a possibility of the application of this combination effect to a therapy of GBM.

Materials and Methods

Primary tumor cultures

Primary GBM surgical specimens were obtained from patients undergoing surgical treatment for newly diagnosed GBM at Shiga Medical Center. This study was approved by the Ethical Committee of the Human Research of Shiga Medical Center. The details of the study were explained to patients before they underwent surgery at Shiga Medical Center. Written agreement had been obtained from a patient for the use of the resected tissue for this research, and de-identified tissues were subjected to the analyses in this study. Within 1 h after surgical removal, tumors were washed and enzymatically dissociated into single cells using a neural cell dissociation kit containing papain (Miltenyi Biotec). CSC sphere cells were cultured in NeuroCult NSC Basal Medium (StemCell Technologies, Vancouver, BC, Canada) containing NeuroCult NSC proliferation Supplements (StemCell Technologies), recombinant bFGF and EGF (40 ng/ml each; Peprotech). RI01 and RI02 lines were derived from a 67-year-old man and a 72-year-old man with glioblastoma multiforme, respectively. RI03 and RI08 lines originated from a 77-year-old woman, and 57-year-old woman with glioblastoma multiforme, respectively.

Primary CSC neurospheres were dissociated every 4 to 7 days to facilitate cell growth. To promote differentiation, CSC neurospheres were enzymatically dissociated, seeded on a Matrigel-coated slide chamber (Nunc) cultured in the same medium without bFGF and EGF but in the presence of 1% FCS for 1 or 3 days. All primary cells were used at low (<30) passage number.

Neural stem cell cultures

Normal neural stem cells were isolated from the ganglionic eminences of E14.5 *INK4/Arf*^{-/-} and control embryos. Cells were cultured in NeuroCult NSC Basal Medium (StemCell Technologies, Vancouver, BC, Canada) containing Neurocult NSC proliferation Supplements (StemCell Technologies), recombinant bFGF and EGF (40 ng/ml each; Peprotech). These cells were subsequently infected with EGFRvIII expressing MSCV retrovirus at first passage and treated with puromycin (0.25 μ g/ml) 48 h after infection. To promote differentiation, EGFRvIII-expressing *INK4/Arf*^{-/-} neural stem cells were dissociated from neurospheres, seeded on a Matrigel-coated slide chamber (Nunc) and cultured in the same medium without bFGF and

EGF but in the presence of 1% FCS. Cells were then fixed with 4% PFA for 15 minutes and processed for immunohistochemistry.

Reagents

10058-F4 (Sigma-Aldrich, St Louis, MO) was dissolved in dimethyl sulfoxide. Arsenic trioxide (Sigma Chemical Co. St. Louis, MO) was dissolved in 5 M solution of sodium hydroxide and then its pH was adjusted to 8.0 with hydrochloric acid. The prepared concentrated solutions were added to the culture medium and mixed gently.

Cell viability and Caspase 3/7 assay

Cell viability and caspase3/7 activity were determined using PrestoBlue Cell Viability Reagent and CellEvent Caspase-3/7 Green Detection Reagent (Molecular Probes, Invitrogen), respectively. 12 h before drug treatment, cells were seeded at a density of 1×10^4 cells (100 μ l) per well in a 96-well plate. The plates were incubated with or without drugs for 24, 72, 168 hours. 10 μ l of PrestoBlue and 0.2 μ l of Caspase-3/7 Green Detection Reagent were added to each well and incubated for 30 minutes at 37°C. Fluorescence intensity was determined using a Varioscan Flash plate reader (Thermo Fisher) with an excitation wavelength of 540 nm and an emission wavelength of 590 nm, and an excitation wavelength of 502 nm and an emission wavelength of 530 nm.

Immunohistochemistry of tissue sections

Immunohistochemical staining was performed with primary antibodies for 12h at 4°C after blocking for 1 h at room temperature with 5% donkey serum (Millipore). Then the sections were incubated for 1 h at room temperature with secondary antibodies (Molecular Probes). Primary and secondary antibodies used were anti-Nestin (Abcam), anti-Olig2 (IBL), anti-CD44 (SantaCruz), anti-Tuj1 (R&D), anti-Ki67 (Abcam), anti-GFAP (DAKO) and Alexa488 or Alexa594-conjugated donkey anti mouse or rabbit IgG (Invitrogen). The TUNEL assay was performed using the Apoptag Fluorescein *In Situ* Apoptosis Detection Kit (Millipore). Slides were analyzed with a Leica confocal laser scanning microscope (SP8, Leica).

Animal xenografts and tumor volume measurement

For *in vivo* experiments, CSCs (5×10^4 cells) were implanted intracranially into 10 week-old female C.B17-lcr SCID mice (Charles River). Two months after transplantation, tumor growth was monitored by animal magnetic resonance imaging (MRI) (7.0 T horizontal-bore MR scanner (Unity Inova; Agilent Technologies, Santa Clara, CA). T2-weighted magnetic resonance imaging was performed in TR/TE 1800 /42 ms with 0.8 mm interval. The sizes of brain tumors were measured in the images. Tumor areas were circumscribed on T2-weighted images using ImageJ (<http://imagej.nih.gov/ij/>) and the total tumor volume is the sum of their corresponding areas in cm² multiplied by the MR interplane gap of 0.8 mm. Four days after tumor size measurement, Arsenic Trioxide (2.5 mg/kg), 10058F4 (25mg/Kg) or both were administered to the animals by i.p. injection once a day for 10days. After 10-day drug treatments, tumor sizes were again measured using animal MRI, and they were perfused with 4% PFA, and their brains were removed and processed for analysis. For the purpose of histological tumor volume estimation, the brains were cut into 30 μ m sections and stained with hematoxylin and eosin (HE). Sections were selected at an interval of 210 μ m. Tumor areas were measured using ImageJ. Tumor volumes were calculated by summing the tumor areas of these sections multiplied by the cross-

sectional interval (210 μ m). The institutional animal care and use committee of Shiga Medical Center approved all of the experiments in our study (Permit number: 24–3, 25–3).

Gli reporter gene assay

GBM CSCs were transfected with a Gli luciferase reporter construct (Signal Reporter Assay kits) (SA Biosciences, Frederick, MD, USA) using Lipofectamine2000 (Invitrogen). The medium was replaced with NeuroCult NSC Basal Medium with or without 2 μ M arsenic trioxide or 60 μ M 10058F4. After 24 hrs, cells were subjected to luciferase assay using a luminometer (Varioskan Flash). Normalized luciferase activity (firefly luciferase / sea urchin luciferase ratio) was then compared in each experiment, samples were analyzed in triplicate, and experiments were repeated at least three times.

Results

Arsenic trioxide and 10058F4 induced differentiation of patient-derived GBM CSCs

To confirm previous reports and examine the effects of arsenic trioxide and 10058F4, an inhibitor of c-Myc on the differentiation of a newly derived GBM CSC neurosphere line (RI01; [Materials and Methods](#)), we treated dissociated neurospheres with 2 μ M arsenic trioxide or 60 μ M 10058F4 for three days in differentiating condition. Immuno-fluorescent studies showed that 10058F4 reduced the number of Nestin-positive and Olig2-positive cells and increased GFAP-positive cells (Nestin: $P = 0.021$, Olig2: $P = 0.012$, GFAP: $P = 0.05$ ([Fig 1A](#) and [1B](#))). In contrast, arsenic trioxide decreased the number of GFAP-positive cells ($P = 0.031$) ([Fig 1A](#) and [1B](#))). Astonishingly, 2 μ M arsenic trioxide as well as 10058F4 enhanced differentiation of CSCs to TujI-positive cells (arsenic trioxide: $P = 0.011$, 10058F4: $P = 0.024$, 10058F4-arsenic trioxide: $P = 0.0036$) ([Fig 1A](#) and [1B](#))). These observations were also confirmed by western blotting ([S1A Fig](#)). Similar results were also noted in another 3 human GBM CSC lines (RI02, RI03 and RI08).

Arsenic trioxide enhanced inhibitory effects of 10058F4 on GBM CSC growth

To determine whether arsenic trioxide potentiate 10058F4 effects, we treated GBM CSCs with 2 μ M arsenic trioxide in combination with 60 μ M 10058F4 in differentiating condition. Cell viability assay showed that co-treatment more effectively inhibited GBM CSC cell growth than monotherapy (RI02: $F_{2,33} = 10.81$, $P = 0.0002$, RI08: $F_{2,33} = 8.02$, $P = .0014$) ([Fig 2A](#)). In contrast, this cotreatment did not affect either activation of Caspase-3/7 in apoptotic signaling (RI02: $P = 0.63$, RI08: $P = 0.63$) ([Fig 2B](#)) or the percentages of TUNEL⁺ cells (RI02: $P = 0.97$, RI08: $P = 0.64$) ([Fig 2C](#)), suggesting this interactive effect is not caused by enhanced apoptosis.

It has been reported that a constitutive active mutant of Notch could overcome the effect of arsenic trioxide on GBM CSCs [[18](#)]. To examine whether Notch signaling is involved in this interactive effects, we subjected GBM CSC lines to a 5x 3 doses of 10058F4 (2.4 μ M, 12 μ M, 60 μ M) singly and in combination with 2 μ M arsenic trioxide or 1 μ M DAPT, a Notch signaling inhibitor. The individual and combined survival curve showed that arsenic trioxide but not DAPT enhanced the responsiveness to 10058F4 (RI02: $F_{1,4} = 23.20$, $P = 0.0085$, RI08: $F_{1,4} = 1950.419$, $P = 0.00001$) ([Fig 3](#)). Similar results were also obtained in another 2 GBM CSC lines (RI01, RI03).

Shh signaling is also essential for the maintenance of GBM CSCs and GBM cells often become resistant to Notch inhibitor through the activation of Shh signaling [[20,21](#)]. Next, we

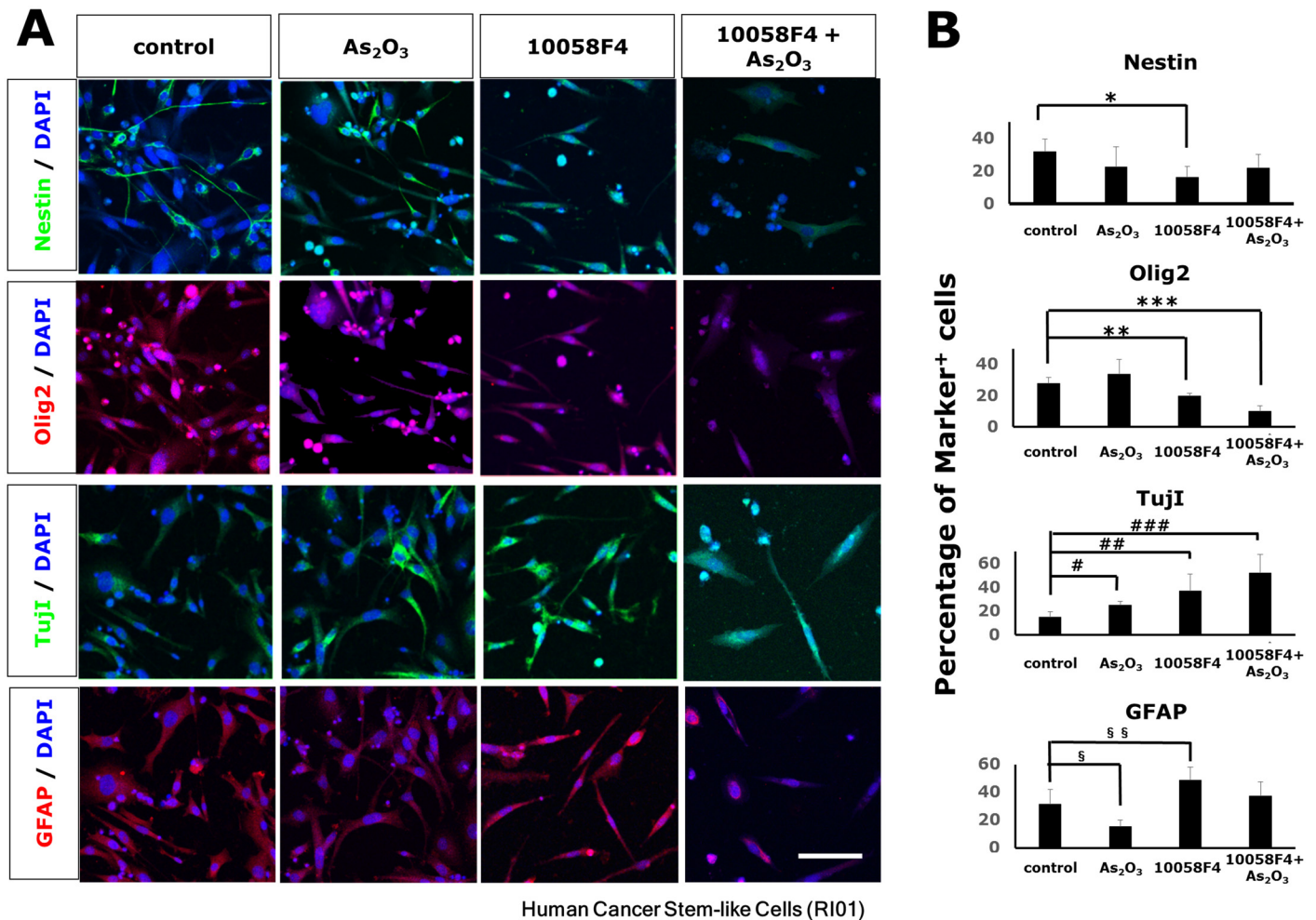


Fig 1. Enhanced differentiation of cancer stem-like cells (CSCs) of glioblastoma multiforme by arsenic trioxide and 10058F4. Immunofluorescent analysis for Nestin (green), Olig2 (red), Tuji1 (green), GFAP (red) and DAPI staining of nuclei (blue) (A) and quantitative analysis of Nestin-positive, Olig2-positive, Tuji1-positive, GFAP-positive cells (B) in cancer stem-like cells (CSCs) of glioblastoma multiforme (GBM) (RI01) 3days after treatment with or without 2µM arsenic trioxide or 60µM 10058F4 in the presence of 1% FCS. Scale bar = 100µm. The data is the mean ± S.D. *P = 0.021, **P = 0.012, ***P = 0.00055, ##P = 0.024, ###P = 0.0036, §P = 0.031, §§P = 0.050.

doi:10.1371/journal.pone.0128288.g001

examined the effects of arsenic trioxide and 10058F4 on Shh signaling in GBM CSCs. Gli reporter assay showed that 10058F4 activated Shh signaling in GBM CSCs but arsenic trioxide did not enhance its effect (Fig 4). Taken together, the effect of this combination therapy seems to be independent of Notch/ Shh signaling. However, off-target effects of these inhibitors are not excluded in this study.

Loss of *Ink4a/Arf* and constitutively activated EGFR enhanced the responsiveness to arsenic trioxide and 10058F4

EGFR activation in *Ink4a/Arf*-deficient astrocytes and neural stem cells (NSCs) is known to provoke GBM-like phenotypes[8]. A constitutively active mutant form of EGFR (EGFRvIII) transforms NSCs into tumorigenic and GBM CSC-like cells. This genetically-defined system provides an opportunity to investigate how EGFR activation with a loss of *Ink4a/Arf* influences the responsiveness of NSCs arsenic trioxide and 10058F4 in differentiating condition. The

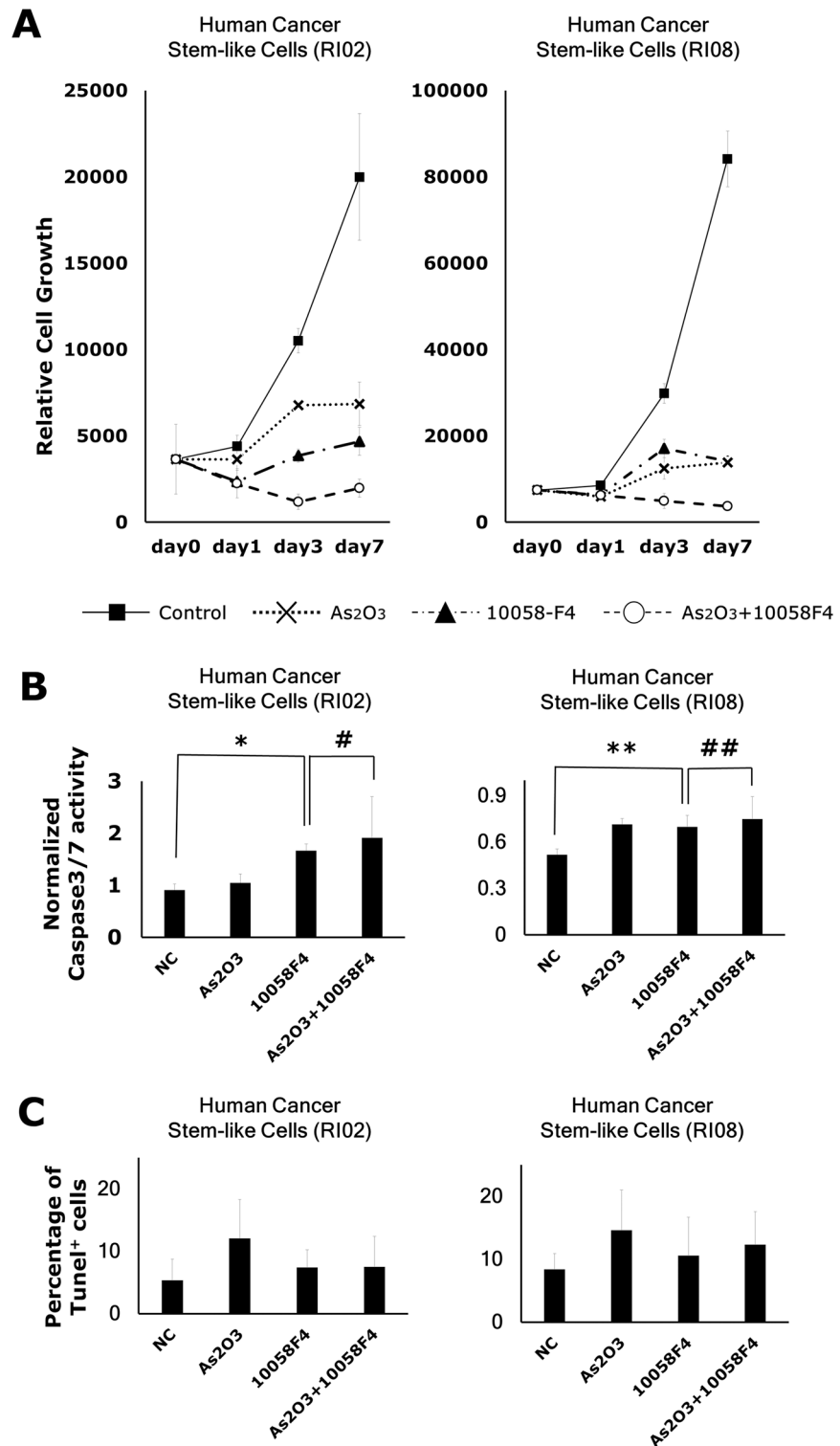


Fig 2. Arsenic trioxide enhanced the inhibitory effect of 10058F4 on GBM CSC growth but not the apoptosis-inducing effect of 10058F4. GBM CSCs (RI02, RI08) were treated with or without 2 μ M arsenic trioxide or 60 μ M 10058F4 for 24, 72 and 168h in the presence of 1% FCS. Results are presented as the relative cell growth (A), the activation of Caspase3/7 (B) and the percentages of TUNEL⁺ cells (C) as determined with PrestoBlue Cell Viability Reagent, CellEvent Caspase-3/7 Green Detection Reagent and TUNEL assay, respectively. Cell viability is presented as the mean \pm SD. The relative fluorescent units of

treated cells were normalized to the cell viability and presented as the mean \pm SD. *P = 0.017, **P = 0.019, #P = 0.72, ##P = 0.43.

doi:10.1371/journal.pone.0128288.g002

differentiation of *Ink4/Arf*^{+/+} NSCs was not affected by 10058F4 (Fig 5A–5C). In contrast, 10058F4 caused an enhanced differentiation of retrovirally EGFRvIII-transduced *Ink4/Arf*^{-/-} NSCs to TujI-positive cells and reduced number of Nestin-positive cells (Nestin: P = 0.00001, TujI: P = 0.0041) (Fig 5A), although arsenic trioxide enhanced TujI-positive cell differentiation of both *Ink4/Arf*^{+/+} NSCs and EGFRvIII-transduced *Ink4/Arf*^{-/-} NSCs (*Ink4/Arf*^{+/+} NSCs: P = 0.00031, EGFRvIII-transduced *Ink4/Arf*^{-/-} NSCs: P = 0.011) (Fig 5B). These results are also confirmed by western blotting (S1B Fig). Cell viability assay showed that EGFR activation and *Ink4/Arf* deficiency increased the sensitivity to co-treatment with arsenic trioxide and 10058F4 but not mono-treatment with 10058F4 (10058F4: genotype x dose interaction, F_{3,15} = 0.53, P = 0.67, arsenic trioxide and 10058F4: genotype x dose interaction, F_{3,12} = 3.95, P = 0.036)

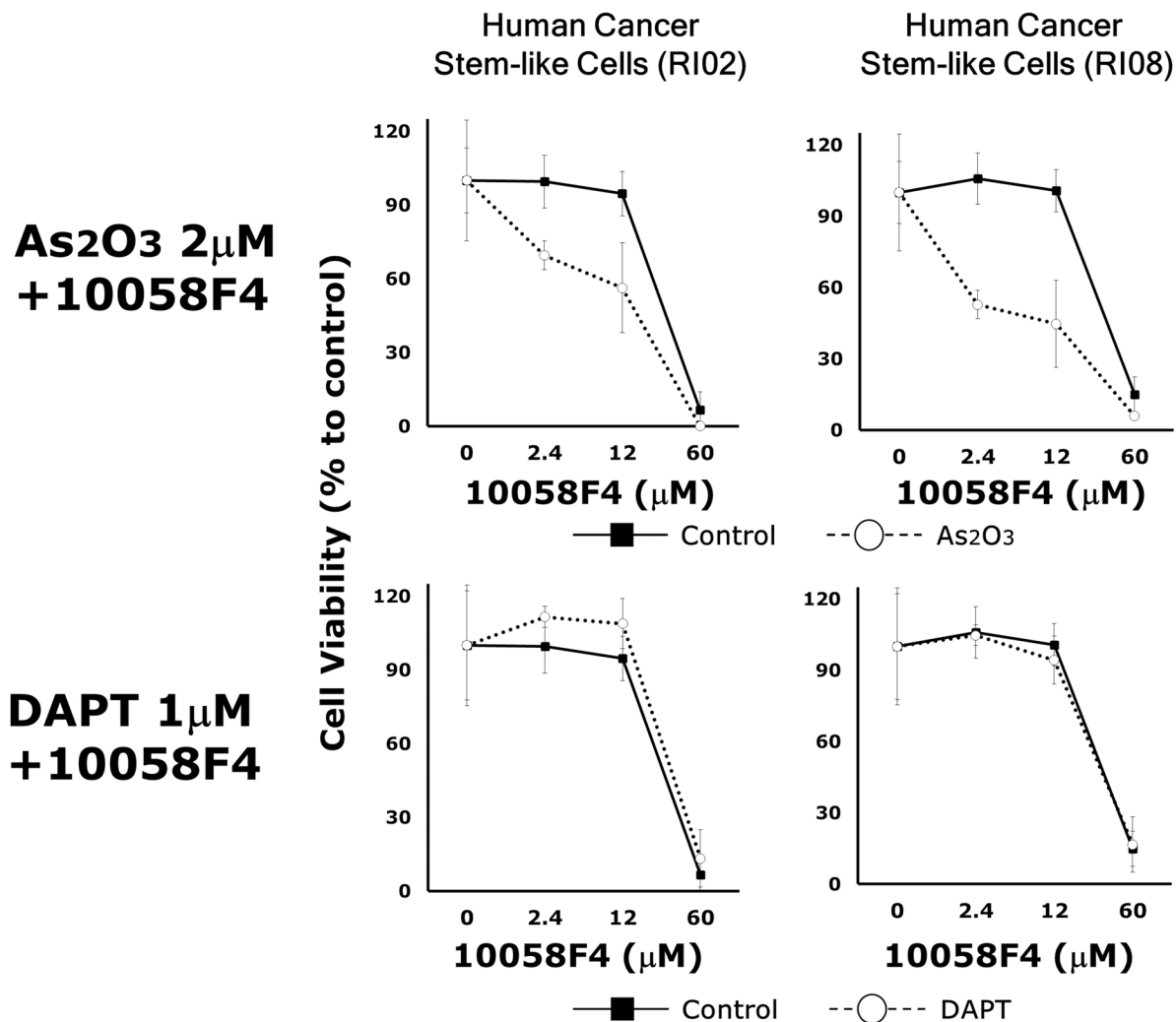


Fig 3. Arsenic trioxide but not DAPT enhanced the responsiveness of GBM CSCs to 10058F4. Dose effects of 10058F4 to GBM CSCs (RI02, RI08) in combination with or without 2 μM arsenic trioxide or 1 μM DAPT for 72h. Results are presented as the relative cell growth as determined with PrestoBlue Cell Viability Reagent. Cell viability is presented as the mean \pm SD.

doi:10.1371/journal.pone.0128288.g003

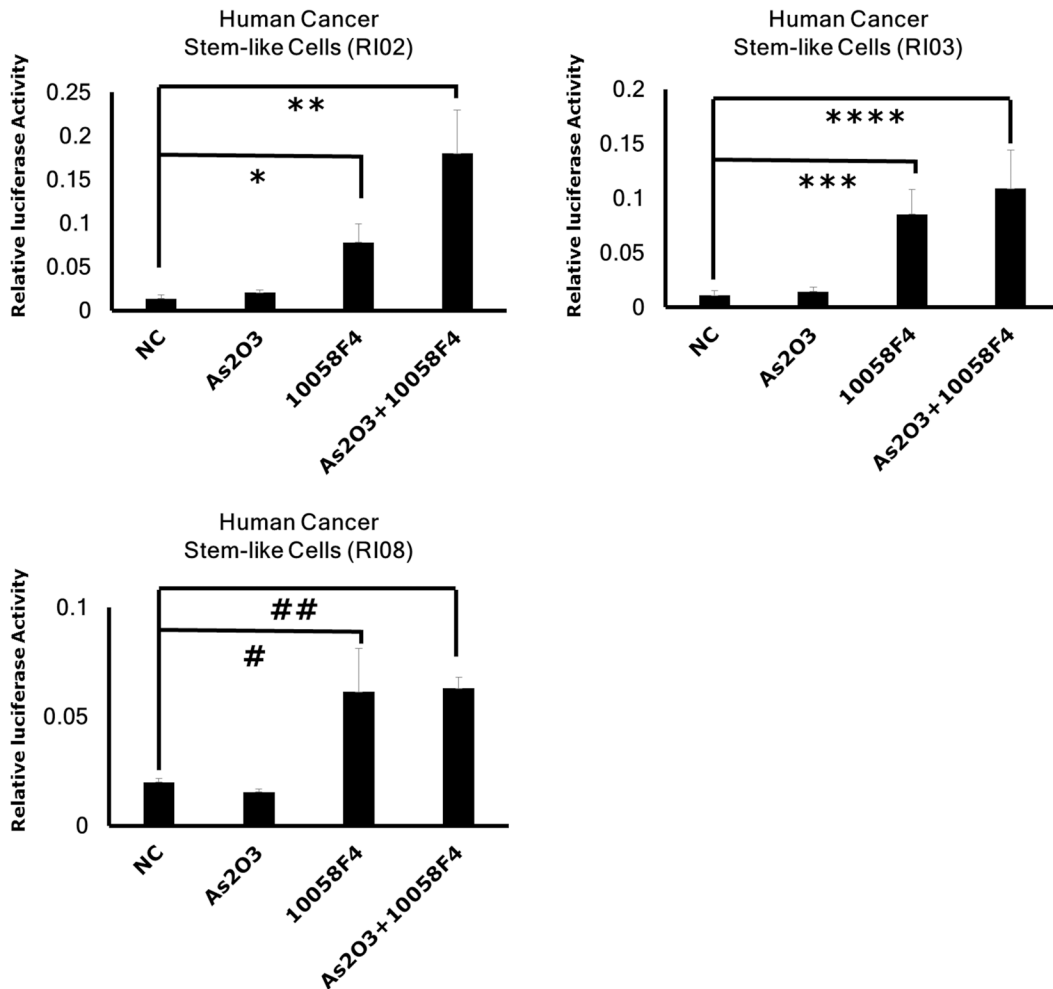


Fig 4. 10058F4 but not arsenic trioxide activated Shh signaling in GBM CSCs. GBM CSCs were transfected with a reporter construct containing a response element for Gli. After 24 hour 10058F4 (60 μ M) and arsenic trioxide (2 μ M) treatment, luciferase assay was performed. Results are the mean \pm S.D. of triplicate data points from a representative experiment. *P = 0.0065 ** P = 0.0043, ***P = 0.0050, ****P = 0.0091, #P = 0.023028, ##P = 0.00015.

doi:10.1371/journal.pone.0128288.g004

(Fig 5D). These findings raise the possibility that arsenic trioxide and 10058F4 combination therapy might be more effective on EGFR-active *Ink4/Arf*-deficient GBM CSCs compared with on normal NSCs.

Arsenic trioxide and 10058 combination treatment blocked glioma progression in a GBM CSC xenograft model

To extend our *in vitro* finding, we studied the effect of arsenic trioxide and 10058F4 on *in vivo* tumor growth and progression using a GBM CSC xenograft model. MRI is a promising noninvasive technique to monitor treatment-induced changes in tumor growth in mice *in vivo* [22]. Tumor volumes derived from MR images were well-correlated with tumor volumes estimated by histological sections ($R = 0.81$, $P = 0.049$) (Fig 6). We assessed initial tumor growth using MRI two months after intracranial injection of GBM CSCs, and randomized implanted mice into arsenic trioxide, 10058F4, both or vehicle cohorts. After 10-day treatment with arsenic trioxide and 10058F4, we reassessed subsequent tumor growth (Fig 7A). Arsenic trioxide and 10058F4 were well tolerated over 10-day treatment with no visible side effects (S2 Fig), which is

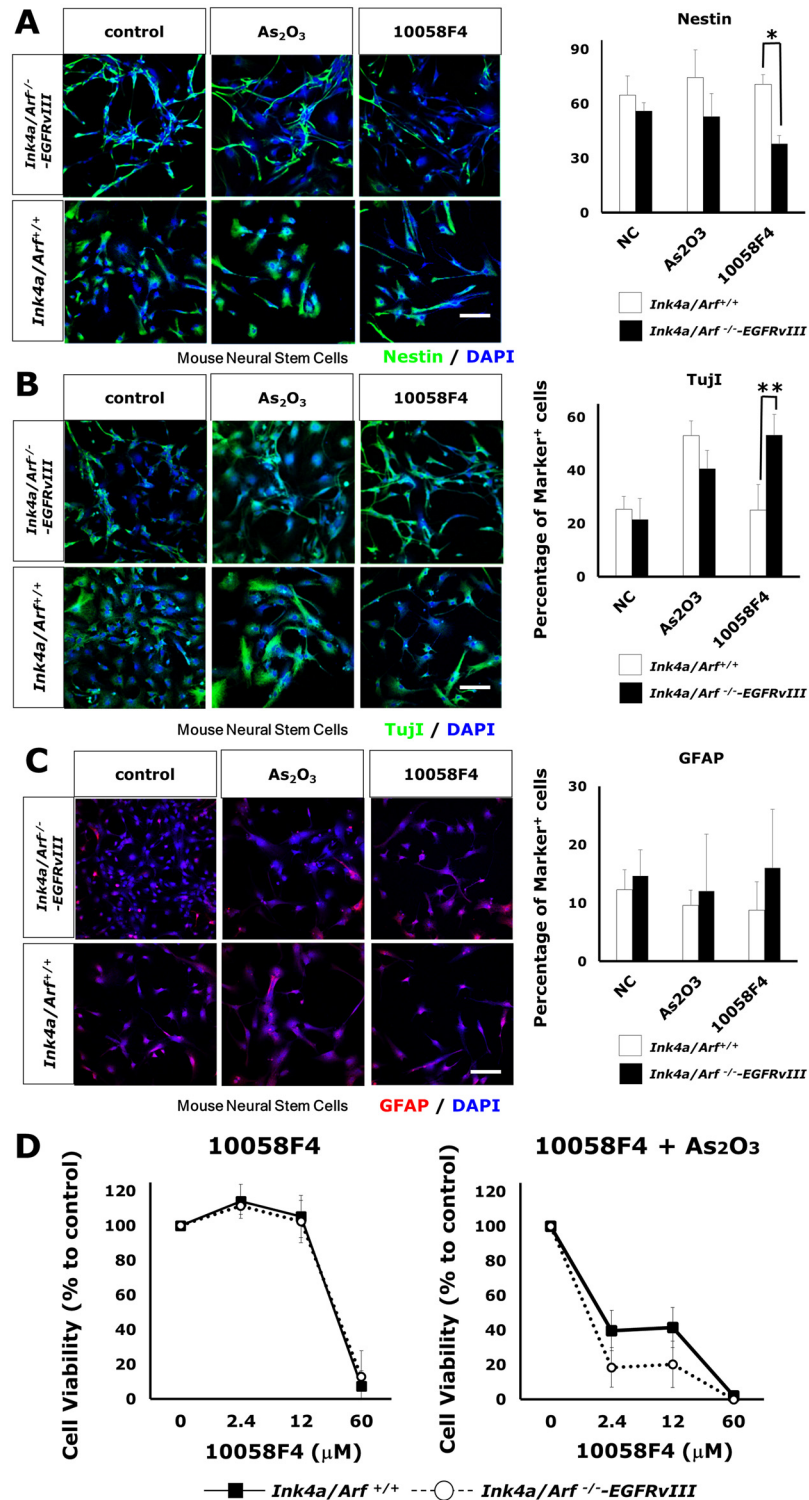


Fig 5. Constitutive activation of EGFR with loss of *Ink4/Arf* enhanced the responsiveness of neural stem cells to arsenic trioxide and 10058F4. (A)-(C) Immunofluorescent analysis for Nestin (green, (A)), Tuji1 (green (B)), GFAP (red (C)) and DAPI staining of nuclei (blue) and quantitative analysis of Nestin-positive (A), Tuji1-positive cells (B), GFAP-positive cells (C) in *Ink4/Arf*^{-/-}-EGFRVIII and control neural stem cells 3days after treatment with or without 2μM arsenic trioxide or 60μM 10058F4. Scale bar = 100μm. The data is the mean ± S.D. *P = 0.00001, **P = 0.0041. (D) Dose effects of 10058F4 to *Ink4/Arf*^{-/-}-EGFRVIII and control neural stem cells in combination with or without 2μM arsenic trioxide for 72h. Results are presented as

the relative cell growth as determined with PrestoBlue Cell Viability Reagent. Cell viability is presented as the mean \pm SD.

doi:10.1371/journal.pone.0128288.g005

consistent with previous reports [23,24]. Arsenic trioxide and 10058F4 combination treatment but not mono-treatment regressed GBM CSC tumor (10058F4: $P = 0.13$, arsenic trioxide: $P = 0.95$, 10058F4-arsenic trioxide: $P = 0.020$, one-way ANOVA, Fisher's LSD test) (Fig 7B–7F and S3 Fig). To determine the mechanism underlying this marked effects of arsenic trioxide and 10058F4 co-treatment, we performed immunohistochemical analysis of treated tumor samples. 10058F4 and cotreatment with arsenic trioxide decreased Ki67-positive proliferating cells (10058F4: $P = 0.016$, 10058F4-arsenic trioxide: $P = 0.0042$) (Fig 8A and 8B). Arsenic trioxide and 10058F4 co-treated mice but not mono-treated mice exhibited drastic reduction of Olig2-positive proneural GBM CSCs and CD44-positive mesenchymal GBM CSCs [25–27] and enhanced differentiation to TujI-positive cells (Olig2: $P = 0.027$, CD44: $P = 0.0075$, TujI: $P = 0.00093$) (Fig 8A and 8B). In addition, 10058F4 increased the number of GFAP-positive cells ($P = 0.00039$), but arsenic trioxide inhibited the effect (Fig 8A and 8B). Thus these data demonstrated that arsenic trioxide and 10058F4 co-treatment induced differentiation of GBM CSCs *in vivo* with concomitant loss of GBM CSCs.

Discussion

Clinical developments of arsenic trioxide and 10058F4, a c-Myc inhibitor are limited due to their low effectiveness, although they have important potential. 10058F4 inhibits c-Myc-mediated transactivation *in vitro*, but failed to show its efficiency *in vivo* except for neuroblastoma models[24,28]. Arsenic trioxide is required to be used at higher concentrations (10–

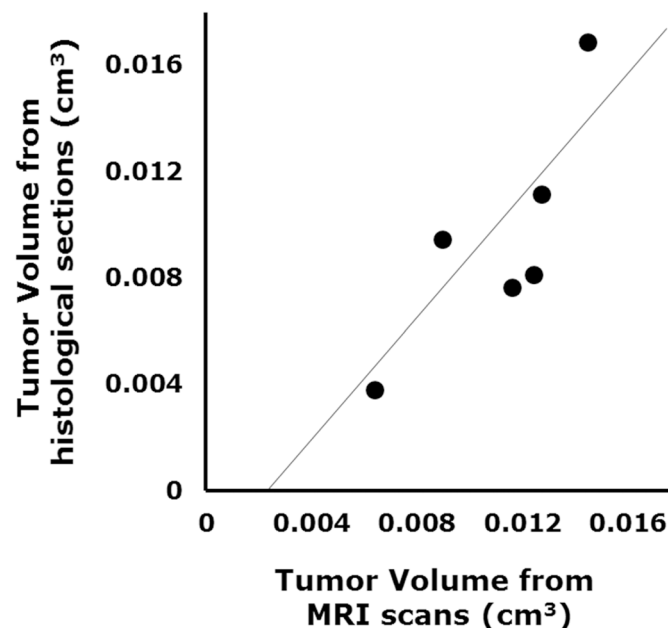


Fig 6. The correlation between tumor volume measurements from MRI scan data and those made from histological sections. GBM CSCs (R103) CSCs (5×10^4 cells) were implanted intracranially into SCID mice. Two months after transplantation, tumor growth was estimated by MRI and histological sections. The correlation coefficient is $R = 0.81$, $P = 0.049$.

doi:10.1371/journal.pone.0128288.g006

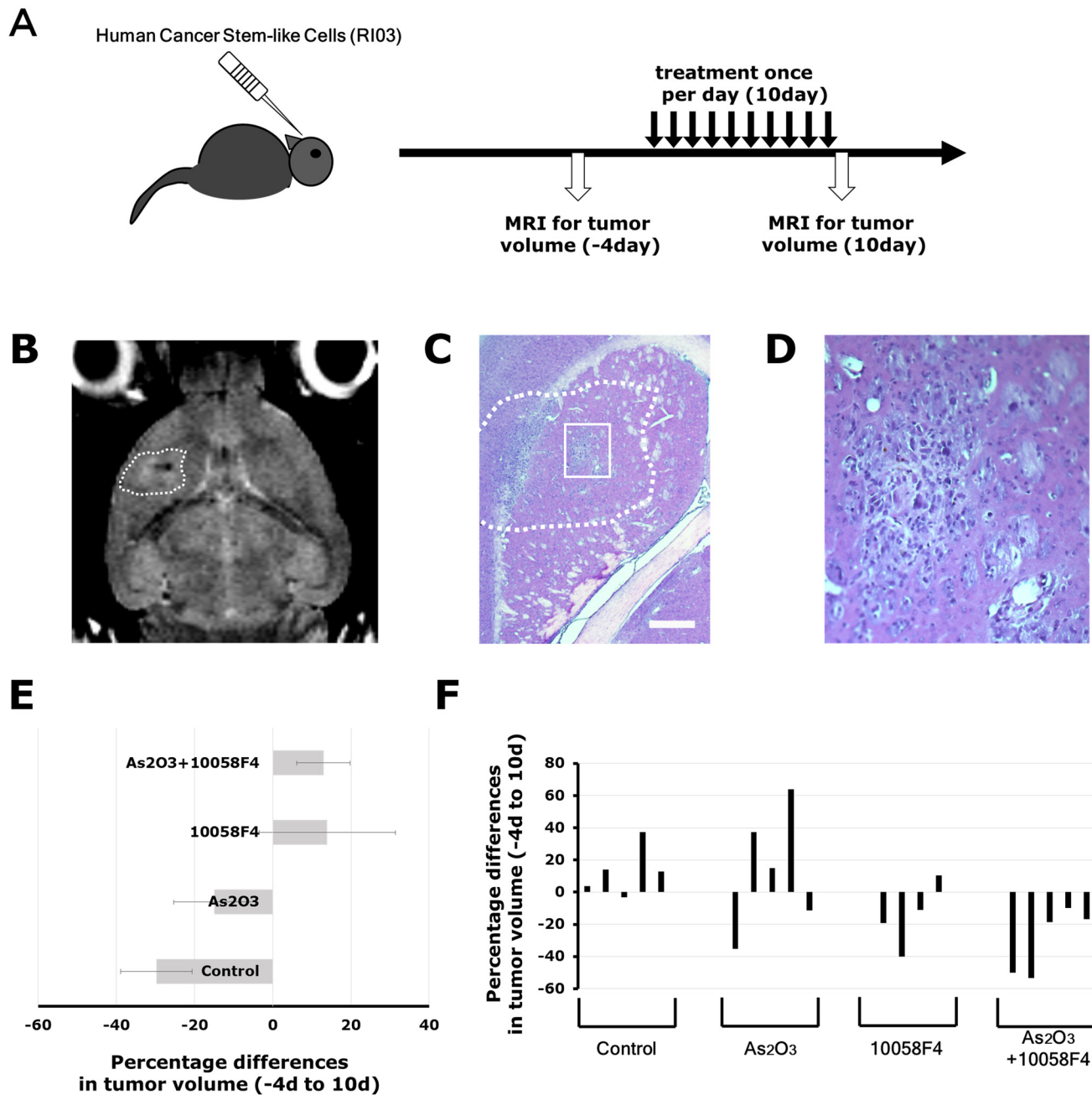


Fig 7. Arsenic trioxide and 10058F4 combination treatment efficiently regressed established gliomas. Experimental Design. GBM CSCs (RI03) CSCs (5×10^4 cells) were implanted intracranially into SCID mice. Two months after transplantation, tumor growth was monitored by MRI. Four days after tumor size measurement, Arsenic Trioxide (2.5 mg/kg), 10058F4 (25mg/Kg) or both were administered by i.p. injection once a day for 10 days. After 10-day drug treatments, tumor sizes were again measured. Representative images of T2-weighted MRI. The region of interest used to calculate the volume of brain tumor is indicated by a dashed line. (C)-(D) Representative photographs of hematoxylin / eosin staining of intracranial xenograft brain tumors. The boxed area in (C) is magnified in (D). Scale bar = 500 μ m. (E)-(F) Changes in tumor volume after 10-day treatment with arsenic trioxide and 10058F4 relative to the starting tumor volume for each individual mouse. Each bar represents a volume change of an individual mouse. The data in (E) is shown as the mean \pm SD of the data for each individual mouse in (F).

doi:10.1371/journal.pone.0128288.g007

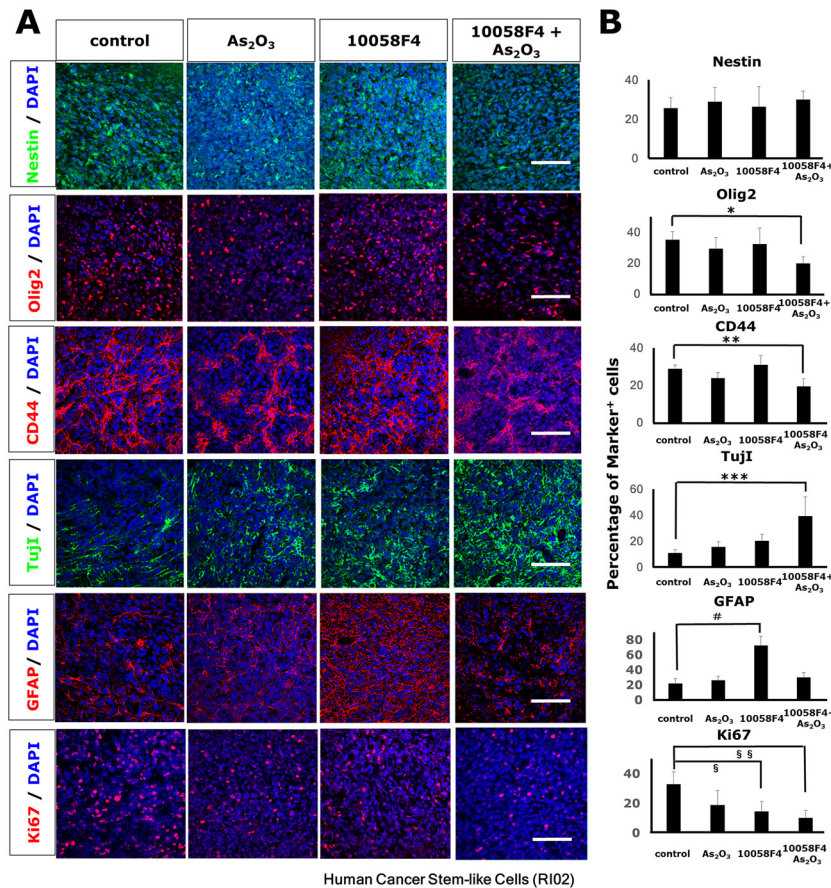


Fig 8. Arsenic trioxide and 10058F4 combination treatment reduced proneural/mesenchymal GBM CSC and induced differentiation to Tuj1-positive cells in a human GBM CSC xenograft model. SCID mice were injected intracranially with 5×10^4 GBM CSCs (RI02). Treatment with arsenic Trioxide (2.5 mg/kg), 10058F4 (25mg/Kg) or both was initiated after the confirmation of tumor growth with MRI and continued daily for 10days. Representative images from 10-day trial in a human GBM CSC xenograft model (A). Immunofluorescent analysis for Nestin (green), Olig2 (red), CD44 (red), Tuj1 (green), GFAP (re), Ki67 (red) and DAPI staining of nuclei (blue) (A) and quantitative analysis of Nestin-positive, Olig2-positive, CD44-positive, Tuj1-positive, GFAP-positive, Ki67-positive cells (B). Scale bar = 100 μ m. The data is the mean \pm S.D. *P = 0.05, **P = 0.001, ***P = 0.001, #P = 0.00039, §P = 0.015847, §§P = 0.0042.

doi:10.1371/journal.pone.0128288.g008

50 μ M) than its safety limit for effective treatment of GBM *in vivo* [14–18]. Our results demonstrated that a low concentration of arsenic trioxide (2 μ M) enhanced the sensitivity of GBM CSCs to 10058F4 and that arsenic trioxide and 10058F4 combination treatment enhanced differentiation of GBM CSCs. This preclinical efficacy of arsenic trioxide and 10058F4 combination therapy were confirmed across multiple GBM models: human GBM CSCs, genetically-engineered mice GBM model, and human-derived GBM CSC xenografts *in vivo*.

Arsenic trioxide and 10058F4 have been reported to regulate metabolic pathways, which play pivotal roles to balance quiescence and proliferation of various types of CSCs. Maintenance of various stem cells including CSCs relies on anaerobic glycolysis, glutamine metabolism and fatty acid metabolism for their survival and proliferation[29–31]. Stem cells and cancer cells uptake glucose at a high rate and convert the majority of it to lactate[32]. This aerobic glycolysis enables an efficient supply of macromolecules for proliferation. In GBM cells, phosphoinositol 3 kinase (PI3K)/Akt signaling and a constitutive active form of EGFR, EGFRvIII promote this glycolytic metabolism through c-Myc regulation [33–35]. EGFRvIII activates

c-Myc signaling through the control of alternative splicing of Max, a Myc binding partner, and mTORC2-dependent upregulation of c-Myc expression level [34,35]. However, when glucose metabolism is limited, glutaminolysis and fatty acid consumption are essential for the survival of cancer cells [36]. Glutaminolysis is also regulated by c-Myc signaling in neuroblastoma cells [36–38]. c-Myc coordinates the expression of the genes necessary for glutaminolysis. c-Myc diverts glucose-derived pyruvate into lactate from tricarboxylic acid cycle (TCA cycle) by induction of lactate dehydrogenase A (LDH-A). As a result, glucose carbon is completely away from mitochondria, and glutamine is essential to maintain TCA cycle activity, which made c-Myc-transformed cells susceptible to inhibition of mitochondrial electron transport chain [36,39], which might explain cooperative effects of 10058F4 with arsenic trioxide, because arsenic trioxide is a mitochondrial toxin [40,41]. A c-Myc regulator, the zinc finger and X-linked transcription factor (ZFX) is indispensable for CSC self-renewal in GBM and AML. ZFX deficiency leads to loss of CSC properties, which can be partially rescued by overexpression of mitochondrial enzymes, Ptpmt1 and Idh2 [42,43]. This finding also suggests the important roles of ZFX-induced c-Myc in mitochondrial functions.

Arsenic trioxide has been shown to induce promyelocytic leukemia protein (PML) degradation [12,44]. PML promotes fatty acid oxidation through activation of peroxidase proliferator-activated receptor (PPAR) signaling [45]. Myc can also promote fatty acid synthesis and fatty acid oxidation [24,39,46]. Fatty acid oxidation provides acetyl-coA to maintain TCA cycle. GBM with EGFR activation is highly dependent on fatty acid synthesis and fatty acid oxidation for survival [47,48]. It is tempting to speculate that fatty acid synthesis and oxidation might be another target of arsenic trioxide and 10058F4 combination therapy. PML is a member of the tripartite motif (TRIM) family and involved in protein degradation through SUMOylation and ubiquitination [49]. It has been reported that PML affects stabilization of c-Myc in AML cells [50]. Another member of TRIM, TRIM3 is a tumor-suppressor of GBM [51]. This protein degradation machinery might be another target of arsenic trioxide.

In summary, we demonstrated an effective pharmacological partnership between arsenic trioxide and c-Myc inhibition that enhanced differentiation of GBM CSCs and regressed GBM CSC tumor growth *in vivo*. These observations provide a foundations for further studies of arsenic trioxide-10058F4 combination therapy for GBM.

Supporting Information

S1 Fig. Quantification of Olig2, TujI and β -Actin in GBM CSCs and *Ink4/Arf*^{-/-}—EGFRvIII neural stem cells. Western blots showing Olig2, TujI and β -Actin levels in GBM CSCs (RI01) (A) and *Ink4/Arf*^{-/-}—EGFRvIII neural stem cells (B) 1 day after treatment with or without 2 μ M arsenic trioxide or 60 μ M 10058F4. (TIF)

S2 Fig. As₂O₃ and 10058F4 are well tolerated for 10-day treatment. As₂O₃ (2.5 mg/kg) and 10058F4 (25mg/Kg) treatment are well-tolerated for up to 10 days (endpoint for this study). Mean weight for 5 male mice over the 10-day trial. Mice were divided by treatment group: control, As₂O₃, 10058F4 and both. After the trial, these mice did not show any obvious macroscopic symptoms. (TIF)

S3 Fig. The effects of Arsenic trioxide and 10058F4 combination treatment. (A) Representative images of T2-weighted MRI. The region of interest used to calculate the volume of brain tumor is indicated by a dashed line. GBM CSCs (RI03) CSCs (5×10^4 cells) were implanted intracranially into SCID mice. Two months after transplantation, tumor growth was monitored

by MRI. Four days after tumor size measurement, Arsenic Trioxide (2.5 mg/kg), 10058F4 (25mg/Kg) or both were administered by i.p. injection once a day for 10days. After 10-day drug treatments, tumor sizes were again measured. (B)–(C) Representative photographs of hematoxylin / eosin staining of intracranial xenograft brain tumors. The boxed area in (B) is magnified in (C). Scale bar = 500µm.

(TIF)

Acknowledgments

This work was supported by Sagawa Foundation (K.T.) and Yasuda Medical Foundation (K.T.).

Author Contributions

Conceived and designed the experiments: AS KN KT. Performed the experiments: YY AS KM TI KT. Analyzed the data: YY AS KM KT. Contributed reagents/materials/analysis tools: TF SY TS MF MS MH SM NO HS. Wrote the paper: YY KT.

References

1. Libermann TA, Nusbaum HR, Razon N, Kris R, Lax I, Soreq H, et al. Amplification, enhanced expression and possible rearrangement of EGF receptor gene in primary human brain tumours of glial origin. *Nature*. 1985; 313(5998):144–7. PMID: [2981413](#).
2. Wong AJ, Bigner SH, Bigner DD, Kinzler KW, Hamilton SR, Vogelstein B. Increased expression of the epidermal growth factor receptor gene in malignant gliomas is invariably associated with gene amplification. *Proc Natl Acad Sci U S A*. 1987; 84(19):6899–903. PMID: [3477813](#).
3. Nishikawa R, Ji XD, Harmon RC, Lazar CS, Gill GN, Cavenee WK, et al. A mutant epidermal growth factor receptor common in human glioma confers enhanced tumorigenicity. *Proc Natl Acad Sci U S A*. 1994; 91(16):7727–31. PMID: [8052651](#).
4. Ekstrand AJ, Longo N, Hamid ML, Olson JJ, Liu L, Collins VP, et al. Functional characterization of an EGF receptor with a truncated extracellular domain expressed in glioblastomas with EGFR gene amplification. *Oncogene*. 1994; 9(8):2313–20. PMID: [8036013](#).
5. Verhaak RG, Hoadley KA, Purdom E, Wang V, Qi Y, Wilkerson MD, et al. Integrated genomic analysis identifies clinically relevant subtypes of glioblastoma characterized by abnormalities in PDGFRA, IDH1, EGFR, and NF1. *Cancer Cell*. 2010; 17(1):98–110. PMID: [20129251](#). doi: [10.1016/j.ccr.2009.12.020](#)
6. Labuhn M, Jones G, Speel EJ, Maier D, Zweifel C, Gratzl O, et al. Quantitative real-time PCR does not show selective targeting of p14(ARF) but concomitant inactivation of both p16(INK4A) and p14(ARF) in 105 human primary gliomas. *Oncogene*. 2001; 20(9):1103–9. PMID: [11314047](#).
7. Hayashi Y, Ueki K, Waha A, Wiestler OD, Louis DN, von Deimling A. Association of EGFR gene amplification and CDKN2 (p16/MTS1) gene deletion in glioblastoma multiforme. *Brain Pathol*. 1997; 7(3):871–5. PMID: [9217972](#).
8. Bachoo RM, Maher EA, Ligon KL, Sharpless NE, Chan SS, You MJ, et al. Epidermal growth factor receptor and Ink4a/Arf: convergent mechanisms governing terminal differentiation and transformation along the neural stem cell to astrocyte axis. *Cancer Cell*. 2002; 1(3):269–77. PMID: [12086863](#).
9. Singh SK, Hawkins C, Clarke ID, Squire JA, Bayani J, Hide T, et al. Identification of human brain tumour initiating cells. *Nature*. 2004; 432(7015):396–401. PMID: [15549107](#).
10. Lee J, Kotliarova S, Kotliarov Y, Li A, Su Q, Donin NM, et al. Tumor stem cells derived from glioblastomas cultured in bFGF and EGF more closely mirror the phenotype and genotype of primary tumors than do serum-cultured cell lines. *Cancer Cell*. 2006; 9(5):391–403. PMID: [16697959](#).
11. Shen ZX, Chen GQ, Ni JH, Li XS, Xiong SM, Qiu QY, et al. Use of arsenic trioxide (As₂O₃) in the treatment of acute promyelocytic leukemia (APL): II. Clinical efficacy and pharmacokinetics in relapsed patients. *Blood*. 1997; 89(9):3354–60. PMID: [9129042](#).
12. Chen GQ, Zhu J, Shi XG, Ni JH, Zhong HJ, Si GY, et al. In vitro studies on cellular and molecular mechanisms of arsenic trioxide (As₂O₃) in the treatment of acute promyelocytic leukemia: As₂O₃ induces NB4 cell apoptosis with downregulation of Bcl-2 expression and modulation of PML-RAR alpha/PML proteins. *Blood*. 1996; 88(3):1052–61. PMID: [8704214](#).

13. Maeda H, Hori S, Nishitoh H, Ichijo H, Ogawa O, Kakehi Y, et al. Tumor growth inhibition by arsenic trioxide (As₂O₃) in the orthotopic metastasis model of androgen-independent prostate cancer. *Cancer Res.* 2001; 61(14):5432–40. PMID: [11454688](#).
14. Ning S, Knox SJ. Increased cure rate of glioblastoma using concurrent therapy with radiotherapy and arsenic trioxide. *Int J Radiat Oncol Biol Phys.* 2004; 60(1):197–203. PMID: [15337556](#).
15. Zhen Y, Zhao S, Li Q, Li Y, Kawamoto K. Arsenic trioxide-mediated Notch pathway inhibition depletes the cancer stem-like cell population in gliomas. *Cancer Lett.* 2010; 292(1):64–72. PMID: [19962820](#). doi: [10.1016/j.canlet.2009.11.005](#)
16. Kanzawa T, Kondo Y, Ito H, Kondo S, Germano I. Induction of autophagic cell death in malignant glioma cells by arsenic trioxide. *Cancer Res.* 2003; 63(9):2103–8. PMID: [12727826](#).
17. Haga N, Fujita N, Tsuruo T. Involvement of mitochondrial aggregation in arsenic trioxide (As₂O₃)-induced apoptosis in human glioblastoma cells. *Cancer Sci.* 2005; 96(11):825–33. PMID: [16271077](#).
18. Wu J, Ji Z, Liu H, Liu Y, Han D, Shi C, et al. Arsenic trioxide depletes cancer stem-like cells and inhibits repopulation of neurosphere derived from glioblastoma by downregulation of Notch pathway. *Toxicol Lett.* 2013; 220(1):61–9. PMID: [23542114](#). doi: [10.1016/j.toxlet.2013.03.019](#)
19. Wang J, Wang H, Li Z, Wu Q, Lathia JD, McLendon RE, et al. c-Myc is required for maintenance of glioma cancer stem cells. *PLoS One.* 2008; 3(11):e3769. PMID: [19020659](#). doi: [10.1371/journal.pone.0003769](#)
20. Schreck KC, Taylor P, Marchionni L, Gopalakrishnan V, Bar EE, Gaiano N, et al. The Notch target Hes1 directly modulates Gli1 expression and Hedgehog signaling: a potential mechanism of therapeutic resistance. *Clin Cancer Res.* 2010; 16(24):6060–70. PMID: [21169257](#). doi: [10.1158/1078-0432.CCR-10-1624](#)
21. Takezaki T, Hide T, Takanaga H, Nakamura H, Kuratsu J, Kondo T. Essential role of the Hedgehog signaling pathway in human glioma-initiating cells. *Cancer Sci.* 2011; 102(7):1306–12. PMID: [21453386](#). doi: [10.1111/j.1349-7006.2011.01943.x](#)
22. Pyonteck SM, Akkari L, Schuhmacher AJ, Bowman RL, Sevenich L, Quail DF, et al. CSF-1R inhibition alters macrophage polarization and blocks glioma progression. *Nat Med.* 2013; 19(10):1264–72. Epub 2013/09/24 06:00. PMID: [24056773](#). doi: [10.1038/nm.3337](#)
23. Iwanami A, Gini B, Zanca C, Matsutani T, Assuncao A, Nael A, et al. PML mediates glioblastoma resistance to mammalian target of rapamycin (mTOR)-targeted therapies. *Proc Natl Acad Sci U S A.* 2013; 110(11):4339–44. PMID: [23440206](#). doi: [10.1073/pnas.1217602110](#)
24. Zirath H, Frenzel A, Oliynyk G, Segerstrom L, Westermark UK, Larsson K, et al. MYC inhibition induces metabolic changes leading to accumulation of lipid droplets in tumor cells. *Proc Natl Acad Sci U S A.* 2013; 110(25):10258–63. PMID: [23733953](#). doi: [10.1073/pnas.1222404110](#)
25. Ligon KL, Huillard E, Mehta S, Kesari S, Liu H, Alberta JA, et al. Olig2-regulated lineage-restricted pathway controls replication competence in neural stem cells and malignant glioma. *Neuron.* 2007; 53(4):503–17. PMID: [17296553](#).
26. Jijiwa M, Demir H, Gupta S, Leung C, Joshi K, Orozco N, et al. CD44v6 regulates growth of brain tumor stem cells partially through the AKT-mediated pathway. *PLoS One.* 2011; 6(9):e24217. PMID: [21915300](#). doi: [10.1371/journal.pone.0024217](#)
27. Bhat KP, Balasubramanian V, Vaillant B, Ezhilarasan R, Hummelink K, Hollingsworth F, et al. Mesenchymal differentiation mediated by NF-kappaB promotes radiation resistance in glioblastoma. *Cancer Cell.* 2013; 24(3):331–46. PMID: [23993863](#). doi: [10.1016/j.ccr.2013.08.001](#)
28. Guo J, Parise RA, Joseph E, Egorin MJ, Lazo JS, Prochownik EV, et al. Efficacy, pharmacokinetics, tissue distribution, and metabolism of the Myc-Max disruptor, 10058-F4 [Z,E]-5-[4-ethylbenzylidene]-2-thioxothiazolidin-4-one, in mice. *Cancer Chemother Pharmacol.* 2009; 63(4):615–25. PMID: [18509642](#). doi: [10.1007/s00280-008-0774-y](#)
29. Takubo K, Nagamatsu G, Kobayashi CI, Nakamura-Ishizu A, Kobayashi H, Ikeda E, et al. Regulation of glycolysis by Pdk functions as a metabolic checkpoint for cell cycle quiescence in hematopoietic stem cells. *Cell Stem Cell.* 2013; 12(1):49–61. PMID: [23290136](#). doi: [10.1016/j.stem.2012.10.011](#)
30. Folmes CD, Nelson TJ, Martinez-Fernandez A, Arrell DK, Lindor JZ, Dzeja PP, et al. Somatic oxidative bioenergetics transitions into pluripotency-dependent glycolysis to facilitate nuclear reprogramming. *Cell Metab.* 2011; 14(2):264–71. PMID: [21803296](#). doi: [10.1016/j.cmet.2011.06.011](#)
31. Pattappa G, Thorpe SD, Jegard NC, Heywood HK, de Bruijn JD, Lee DA. Continuous and uninterrupted oxygen tension influences the colony formation and oxidative metabolism of human mesenchymal stem cells. *Tissue Eng Part C Methods.* 2013; 19(1):68–79. PMID: [22731854](#). doi: [10.1089/ten.TEC.2011.0734](#)
32. Warburg O. On the origin of cancer cells. *Science.* 1956; 123(3191):309–14. PMID: [13298683](#).

33. Elstrom RL, Bauer DE, Buzzai M, Karnauskas R, Harris MH, Plas DR, et al. Akt stimulates aerobic glycolysis in cancer cells. *Cancer Res.* 2004; 64(11):3892–9. PMID: [15172999](#).
34. Babic I, Anderson ES, Tanaka K, Guo D, Masui K, Li B, et al. EGFR mutation-induced alternative splicing of Max contributes to growth of glycolytic tumors in brain cancer. *Cell Metab.* 2013; 17(6):1000–8. PMID: [23707073](#). doi: [10.1016/j.cmet.2013.04.013](#)
35. Masui K, Tanaka K, Akhavan D, Babic I, Gini B, Matsutani T, et al. mTOR complex 2 controls glycolytic metabolism in glioblastoma through FoxO acetylation and upregulation of c-Myc. *Cell Metab.* 2013; 18(5):726–39. PMID: [24140020](#). doi: [10.1016/j.cmet.2013.09.013](#)
36. Wise DR, DeBerardinis RJ, Mancuso A, Sayed N, Zhang XY, Pfeiffer HK, et al. Myc regulates a transcriptional program that stimulates mitochondrial glutaminolysis and leads to glutamine addiction. *Proc Natl Acad Sci U S A.* 2008; 105(48):18782–7. PMID: [19033189](#). doi: [10.1073/pnas.0810199105](#)
37. Dang CV, Le A, Gao P. MYC-induced cancer cell energy metabolism and therapeutic opportunities. *Clin Cancer Res.* 2009; 15(21):6479–83. PMID: [19861459](#). doi: [10.1158/1078-0432.CCR-09-0889](#)
38. Dang CV, Dang CV, Le A, Gao P. MYC on the path to cancer MYC-induced cancer cell energy metabolism and therapeutic opportunities. *Cell.* 2012; 149(1):22–35. PMID: [22464321](#). doi: [10.1016/j.cell.2012.03.003](#)
39. Fan Y, Dickman KG, Zong WX. Akt and c-Myc differentially activate cellular metabolic programs and prime cells to bioenergetic inhibition. *J Biol Chem.* 2010; 285(10):7324–33. PMID: [20018866](#). doi: [10.1074/jbc.M109.035584](#)
40. Kroemer G, de The H. Arsenic trioxide, a novel mitochondriotoxic anticancer agent? *J Natl Cancer Inst.* 1999; 91(9):743–5. PMID: [10328097](#).
41. Miller WH Jr., Schipper HM, Lee JS, Singer J, Waxman S. Mechanisms of action of arsenic trioxide. *Cancer Res.* 2002; 62(14):3893–903. PMID: [12124315](#).
42. Fang X, Huang Z, Zhou W, Wu Q, Sloan AE, Ouyang G, et al. The zinc finger transcription factor ZFX is required for maintaining the tumorigenic potential of glioblastoma stem cells. *Stem Cells.* 2014; 32(8):2033–47. Epub 2014/05/17 06:00. PMID: [24831540](#). doi: [10.1002/stem.1730](#)
43. Weisberg SP, Smith-Raska MR, Esquilin JM, Zhang J, Arenzana TL, Lau CM, et al. ZFX controls propagation and prevents differentiation of acute T-lymphoblastic and myeloid leukemia. *Cell Rep.* 2014; 6(3):528–40. Epub 2014/02/04 06:00. PMID: [24485662](#). doi: [10.1016/j.celrep.2014.01.007](#)
44. Soignet SL, Maslak P, Wang ZG, Jhanwar S, Calleja E, Dardashti LJ, et al. Complete remission after treatment of acute promyelocytic leukemia with arsenic trioxide. *N Engl J Med.* 1998; 339(19):1341–8. PMID: [9801394](#).
45. Carracedo A, Weiss D, Lelias AK, Bhasin M, de Boer VC, Laurent G, et al. A metabolic prosurvival role for PML in breast cancer. *J Clin Invest.* 2012; 122(9):3088–100. PMID: [22886304](#). doi: [10.1172/JCI62129](#)
46. Morrish F, Noonan J, Perez-Olsen C, Gafken PR, Fitzgibbon M, Kelleher J, et al. Myc-dependent mitochondrial generation of acetyl-CoA contributes to fatty acid biosynthesis and histone acetylation during cell cycle entry. *J Biol Chem.* 2010; 285(47):36267–74. PMID: [20813845](#). doi: [10.1074/jbc.M110.141606](#)
47. Guo D, Prins RM, Dang J, Kuga D, Iwanami A, Soto H, et al. EGFR signaling through an Akt-SREBP-1-dependent, rapamycin-resistant pathway sensitizes glioblastomas to antiproliferative therapy. *Sci Signal.* 2009; 2(101):ra82. PMID: [20009104](#). doi: [10.1126/scisignal.2000446](#)
48. Cvrljevic AN, Akhavan D, Wu M, Martinello P, Furnari FB, Johnston AJ, et al. Activation of Src induces mitochondrial localisation of de2-7EGFR (EGFRvIII) in glioma cells: implications for glucose metabolism. *J Cell Sci.* 2011; 124(Pt 17):2938–50. PMID: [21878501](#). doi: [10.1242/jcs.083295](#)
49. Guo L, Giasson BI, Glavis-Bloom A, Brewer MD, Shorter J, Gitler AD, et al. A cellular system that degrades misfolded proteins and protects against neurodegeneration. *Mol Cell.* 2014; 55(1):15–30. Epub 2014/06/03 06:00. PMID: [24882209](#). doi: [10.1016/j.molcel.2014.04.030](#)
50. Buschbeck M, Urbesalgo I, Ledl A, Gutierrez A, Minucci S, Muller S, et al. PML4 induces differentiation by Myc destabilization. *Oncogene.* 2007; 26(23):3415–22. Epub 2006/12/06 09:00. PMID: [17146439](#).
51. Chen G, Kong J, Tucker-Burden C, Anand M, Rong Y, Rahman F, et al. Human Brat ortholog TRIM3 is a tumor suppressor that regulates asymmetric cell division in glioblastoma. *Cancer Res.* 2014; 74(16):4536–48. Epub 2014/06/21 06:00. PMID: [24947043](#). doi: [10.1158/0008-5472.CAN-13-3703](#)